

Crystallization behavior of hyperbranched polyethylenes with different degree of branching

Xiang Luo, Wei Huang, Deyue Yan

School of Chemistry and Chemical Engineering, State Key Laboratory of Metal Matrix Composites, Shanghai Jiao Tong University, 800 Dongchuan Road, Shanghai 200240, China

Correspondence to: W. Huang (E-mail: hw66@sjtu.edu.cn)

ABSTRACT: Hyperbranched polyethylenes (HBPEs) with different degree of branching (DB) and similar M_n are used to investigate the effect of branch structure on their crystallization behaviors. The crystal structure, isothermal, and non-isothermal crystallization kinetics of HBPEs are studied by X-ray diffraction and differential scanning calorimetry. The isothermal crystallization process is analyzed by the Avrami equation while the non-isothermal crystallization process is analyzed through the Ozawa and Mo methods. The XRD results indicate that the crystallization ability of HBPEs is weakened with the introduction of branch structure, i.e., the crystallinity of HBPEs decreases with the increase of DB, and even tends to zero. The kinetics results of isothermal and non-isothermal crystallization verify the peculiar effects of DB on the crystallization process of HBPEs. In detail, a little of branch structure can accelerate the crystallization process of HBPEs, however a large number of branch can inhibit it. © 2016 Wiley Periodicals, Inc. *J. Appl. Polym. Sci.* **2016**, *133*, 44127.

KEYWORDS: crystallization; dendrimers; hyperbranched polymers and macrocycles; polyolefins

Received 10 March 2016; accepted 25 June 2016

DOI: 10.1002/app.44127

INTRODUCTION

In recent decades, hyperbranched polymers (HBPs) have drawn extensive attention because of their wide applications in various fields, for example, light emitting materials,^{1,2} nanoscience and technology,^{3,4} supramolecular chemistry,^{5,6} biomaterials,^{7,8} hybrid materials and composites,^{9,10} coatings,^{11,12} adhesives,^{13,14} and modifiers.^{15,16} HBPs have exhibited many intriguing physical and chemical properties benefiting from their highly branched architecture with plenty of terminal groups, inner cavities, and lack of chain entanglements.^{17–24} Crystallization is one of the most important properties which affect the physical properties of polymers. For a linear polymer, the molecular chains are easy to rearrange and the crystallization degree is usually very high to provide strength for industry application. But for HBPs, their crystallization ability is poor because their highly branched structure makes the chain rearrangement very difficult to take place. Recently we synthesized a series of HBPEs and studied the effects of DB on their glass transition temperature.²⁵ Simultaneously, we also found most of them still had crystallization ability. It is essential to investigate the crystallization kinetics and melting behavior of HBPEs for its potential applications in the future.

Actually crystallization behaviors of polymers with branches have been studied for many years. For example, Geifer *et al.*²⁶ studied the effect of composition distribution in ethylene- α -olefin copolymers on their solidification behavior during crystallization, they proved that the type of composition distribution rather than the overall content of branched units determined the properties of the copolymers. Chae *et al.*²⁷ investigated the effect of molecular weight and branch structure on the crystallization and rheological properties of poly(butylene adipate). They concluded that the increasing molecular weight retarded the crystallization rate and increased the induction time for crystallization. Introducing branches to the polymer led to similar results. Chiu *et al.*²⁸ discussed the crystallization kinetics of polyethylenes with well-controlled molecular weight and short chain branch (SCB) content. They found that the crystallization temperature and the crystallization rate were dependent on the molecular weight and the short chain branch content. Zhang and coworkers^{29,30} studied the roles of branch content and branch length in copolyethylene crystallization by molecular simulations. They indicated that the branch content played an important role in the crystallization procedure. With the decrease of the branch contents, more perfect lamellar structure was formed and the crystallinity of

Additional Supporting Information may be found in the online version of this article.

© 2016 Wiley Periodicals, Inc.

the copolymer increased. In other words, the crystallinity was inhibited by the increase of branch content. Whereas when the branch length was increased, the branch was folded back and cocrystallized with the main chain. Mai *et al.*³¹ studied the dependence of crystallinity on DB for hyperbranched poly[3-ethyl-3-(hydroxymethyl)oxetane] and found that the crystallinity decreased with increasing DB. The effects of the distribution of SCB on crystallization kinetics of high-density polyethylene was also studied by Krishnaswamy and coworkers.³² They found that the crystallization kinetics of PE products depended on the distribution of branches in addition to molecular weight. Yoshinobu *et al.*³³ studied the unusual crystallization behavior of copolyethylene having precisely spaced branches, they displayed an evidence for a transient ordered mesophase in the crystallization of PE with SCBs. Yang *et al.*³⁴ studied the effect of long chain branching on non-isothermal crystallization behavior of polyethylenes. They found that the long chain branch could limit the chain diffusion and thus decreased the overall crystallization rate. Wang *et al.*³⁵ studied the effects of branches on the crystallization kinetics of polypropylene-*g*-polystyrene. They concluded that the introduction of branch structure restrained the mobility and reptation ability of the polymer backbones, and further hindered the crystallization process. With increasing branch length, the heterogeneous nucleation effect resulting from the branched structure and fluctuation-assisted nucleation mechanism became more pronounced and further facilitated the crystallization process. This meant that a slight amount of branching content might play a role of nucleating agent and accelerate the crystallization process. In summary, there are many factors to affect the crystallization of polymers. Especially when branching is introduced into them, the crystallization process of polymers becomes more complex. Previous reports have mainly focused on the crystallization behavior of linear polyethylene or polyethylene with short or long branches.^{36–39}

In this study, we investigated the relationship of DB and crystallization ability of HBPEs with similar averaged-number molecular weights and various DB. XRD and DSC measurements were adopted to determine the crystal structure and study the isothermal and non-isothermal crystallization kinetics of HBPEs respectively. The isothermal crystallization process was analyzed by Avrami equation while the non-isothermal crystallization process was analyzed through the Ozawa and modified Avrami-Ozawa methods (Mo' equation). These results might provide a potential reference meaning for the future researches.

EXPERIMENTAL

Materials

Four HBPE samples with similar M_n and different DB were prepared in our recent work,²⁵ including HBPE1 ($M_n = 93.6$ kg/mol, DB = 0); HBPE2 ($M_n = 107.3$ kg/mol, DB = 0.110); HBPE3 ($M_n = 110.0$ kg/mol, DB = 0.186; and HBPE4 ($M_n = 100.1$ kg/mol, DB = 0.258).

Characterization

The crystal structure of HBPEs was examined by X-ray diffraction on a Bruker D8 Advance X-ray diffractometer using CuK α radiation at room temperature. The scanning rate was set as 2° min^{-1} in the range of 5° to 70° . Isothermal and non-isothermal crystallization kinetics of HBPEs were studied under

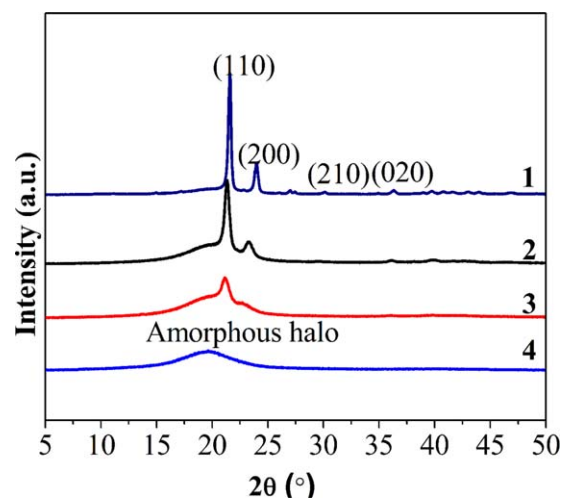


Figure 1. XRD curves of HBPEs with different DB. [Color figure can be viewed in the online issue, which is available at wileyonlinelibrary.com.]

a N_2 atmosphere using a Perkin-Elmer Diamond differential scanning calorimeter (DSC). The amount of HBPE sample was 7.0–8.5 mg for each DSC measurement. For isothermal crystallization, the sample was heated from room temperature to 170°C and held for 5 min to eliminate its thermal history. Subsequently, the sample was cooled to the selected crystallization temperature at $150^\circ\text{C min}^{-1}$; for non-isothermal crystallization, the sample was first heated from -60°C to 170°C at $30^\circ\text{C min}^{-1}$, and held there for 5 min to eliminate its thermal history. Subsequently, the sample was cooled to -60°C at 5, 10, 20, 30 and $40^\circ\text{C min}^{-1}$, respectively.

RESULTS AND DISCUSSION

XRD Analysis

The crystal structure of HBPEs was first investigated by XRD measurement and the resulting XRD patterns were illustrated in Figure 1. Except for HBPE4, other HBPE samples exhibited two distinct major characteristic crystalline peaks at the scattering angles of $2\theta = 21.6$ and $2\theta = 23.9$, which corresponded to the [110] and [200] reflection planes of the orthorhombic crystal structure related to polyethylene, respectively. The obvious difference of the XRD patterns for HBPE samples was that the relative intensity of [110] and [200] reflection peaks ($I[200]/I[110]$). The value of $I[200]/I[110]$ for HBPE samples was decreased with increasing DB, which was in accordance with the results reported by Zhang *et al.*⁴⁰ With increasing the DB, the diffraction peak even disappeared and the amorphous halo (at about $2\theta = 19$) was observed in the XRD pattern of HBPE 4, which implied that the introduction of branching architecture could inhibit the crystallization of polyethylene. In summary, the crystallinity of HBPE samples decreased with the increase of DB. HBPE4 with the high DB eventually became an amorphous polymer.

Equilibrium Melting Temperature

During the DSC measurement, the HBPE samples were heated from the crystallization temperature (T_c) to 170°C at 10°C/min to determine their equilibrium melting temperatures (T_m^0). Figure 2 displayed the DSC melting thermograms of HBPEs with the different DB after isothermal crystallization at various

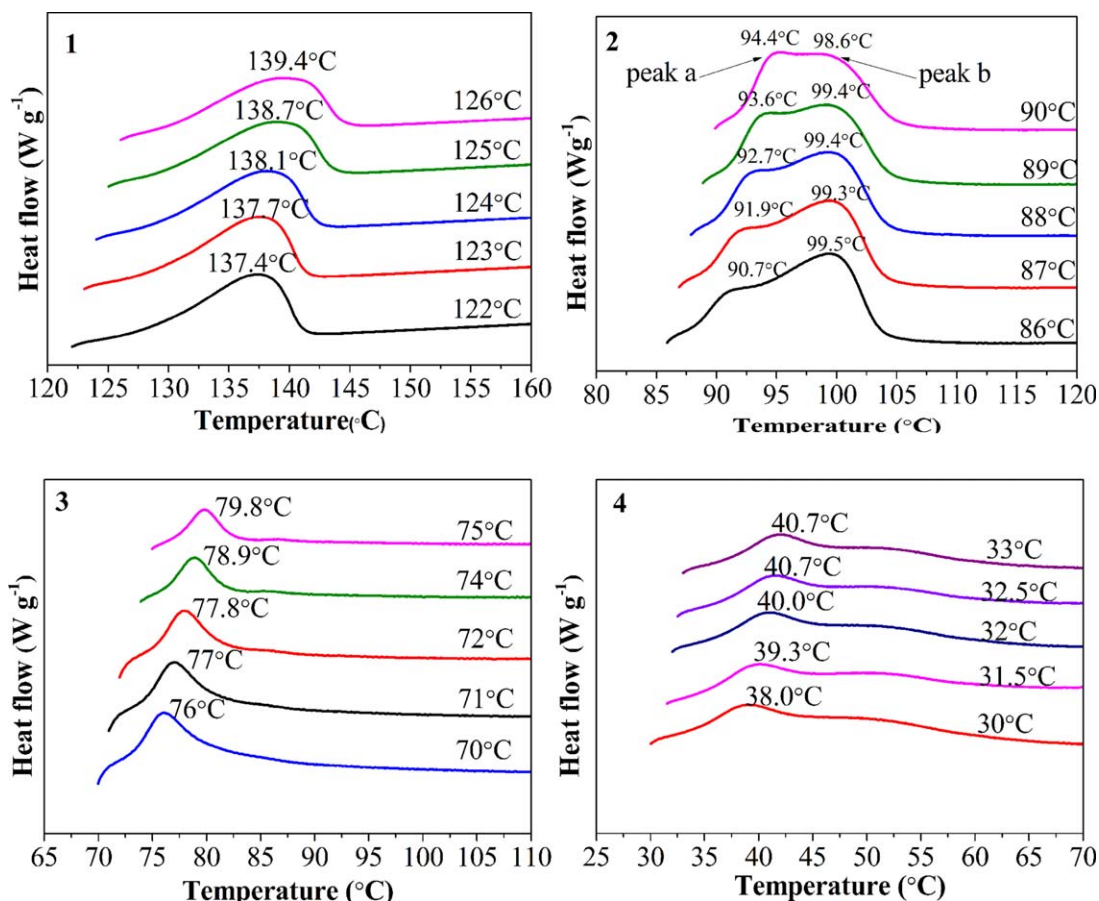


Figure 2. The DSC melting thermograms of HBPEs after isothermal crystallization at various crystallization temperatures. [Color figure can be viewed in the online issue, which is available at wileyonlinelibrary.com.]

crystallization temperatures. The DSC results showed that some crystallization occurred to HBPE4, which was different from that showed through XRD results. Except for HBPE2, all the DSC curves of other HBPEs exhibit a single melting peak. There are two peaks (peak a and b) appeared on the DSC curve of HBPE2. Peak a rises in size and shifts to the higher temperature as the T_c increases. At the same time, peak b becomes smaller but its peak position remains around 99°C. The double melting peaks of HBPE2 can be attributed to recrystallization phenomena during the continuous heating process.^{41–43} Peak a might be the result from the melting of the crystal formed at each crystallization temperature, while peak b may be attributed to the more perfect crystals.

As an important characteristic parameter of the crystal for the flexible linear polymer, T_m^0 illustrated the melting temperature (T_m) of an infinitely extended crystal and could be obtained from the procedure suggested by Hoffman and Weeks.⁴⁴ According to the theoretical considerations by Hoffman and Weeks, the dependence of T_m and T_c was expressed as follows:

$$T_m = \frac{T_c}{2\beta} + T_m^0 \left[1 - \frac{1}{2\beta} \right] \quad (1)$$

Where β is the lamella thickening factor, which indicates the ratio of the thickness of the mature crystal L_c to that of the initial crystal L_c^* .

The plot of T_m versus T_c are presented in Supporting Information Figure S1. An equilibrium melting temperature (T_m^0) can be obtained by means of the extrapolation of the resulting straight line to the line $T_m = T_c$. T_m^0 of four HBPEs is 152.4, 139.8, 92.9 and 53.2°C, respectively. This indicates that the thickness of the crystal plates decreases with increasing the DB. In other words, the crystallization of HBPEs can be inhibited by the branching structure.

Isothermal Crystallization Kinetics Analysis

Isothermal crystallization was carried out at various temperatures in the vicinity of T_c . Figure 3 showed the isothermal exothermic curves of HBPE samples obtained at different T_c s. The DSC curves for all HBPEs exhibited a single peak, which was characteristic for isothermal polymer crystallization. It was obvious that the crystallization behaviors of HBPEs was strongly affected by the T_c . With increasing T_c , the exothermic peaks shifted to long time values. This indicated that the crystallization rate decreased with increasing the T_c and the time required to reach the maximum degree of crystallization increased. On the other hand, the T_c of HBPEs decreased with increasing DB and the T_c of the linear polyethylene was higher than that of other three HBPEs. Besides, the crystallization peak became flatter with increasing T_c . Therefore, we could speculate that the branch structure of HBPEs brought a negative effect on their isothermal crystallization.

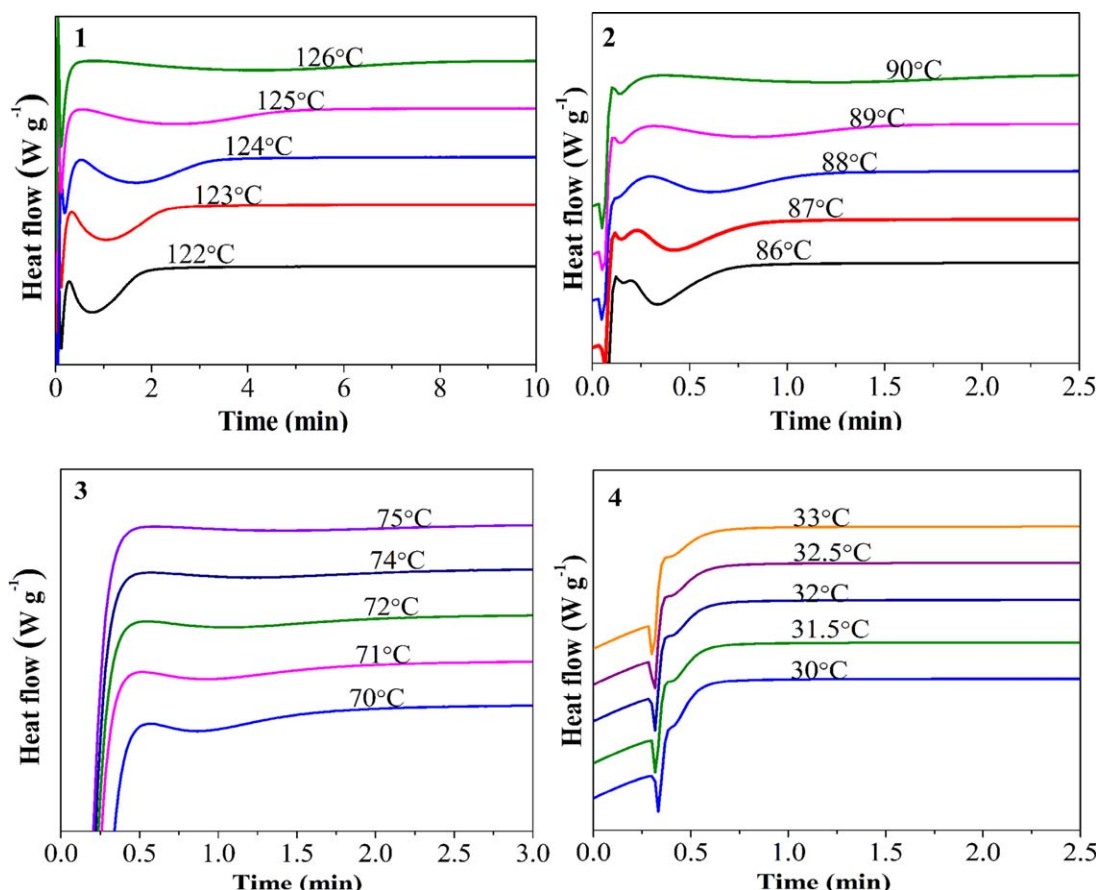


Figure 3. Heat flow versus crystallization time at different crystallization temperatures in isothermal crystallization processes of HBPEs. [Color figure can be viewed in the online issue, which is available at wileyonlinelibrary.com.]

The Avrami equation is well known for analyzing the isothermal crystallization of polymers. So it was employed to quantitatively analyze the isothermal crystallization of HBPEs here. The classical Avrami equation was given as:

$$1 - X_t = \exp(-Kt^n) \quad (2)$$

X_t was the relative crystallinity at time t . K was the crystallization rate constant depending on the nucleation and growth rate. Where n was the Avrami exponent, which was related to the nucleation mechanism and crystal grown dimensions.

Figure 4 showed the time evolution of the relative crystallinity of HBPEs at various temperatures in isothermal crystallization process. Obviously, all the isotherms shifted to the right along the time axis with increasing the crystallization temperature, which indicated the crystallization rate was gradually decreased. This was in accordance with the results in Figure 3.

Equation (2) was converted to

$$\ln[-\ln(1 - X_t)] = \ln K + n \ln t \quad (3)$$

The graphic representation of $\ln[-\ln(1 - X_t)]$ versus $\ln t$ would generate a straight line. Then the Avrami exponent n and crystallization rate constant $K(T)$ was determined from the slope and intercept of the line, respectively. The plots of $\ln[-\ln(1 - X_t)]$ versus $\ln t$ plots were shown in Supporting Information Figure S2. When X_t was equal to 0.5, the Crystallization half-time ($t_{1/2}$) could be

obtained. The $t_{1/2}$ was defined as the time at which the extent of crystallization was 50% and determined from the following equation:

$$t_{1/2} = \left(\frac{\ln 2}{K}\right)^{1/n} \quad (4)$$

Usually, $t_{1/2}$ represented the overall crystallization rate of the polymer. The rate of crystallization, G , was described as the reciprocal of $t_{1/2}$, that is $G = \tau_{1/2} = (t_{1/2})^{-1}$. The necessary time for maximum crystallization, t_{\max} , could be derived from Avrami equation:

$$t_{\max} = \left(\frac{n-1}{nK}\right)^{1/n} \quad (5)$$

The isothermal crystallization kinetic parameters of HBPEs at different crystallization temperature were shown in Table I. The $t_{1/2}$ increased and the K values decreased with increasing crystallization temperature for HBPEs. This indicated the crystallization was retarded by the high temperature. However, the values of n were almost unchanged at different crystallization temperatures for each sample, which implied the crystallization mechanism did not change in the investigated crystallization temperature range. All the values of Avrami exponent n were between 2 and 3, and similar to the report of Jonsson *et al.*,⁴⁵ i.e., a mixed nucleation and crystal growth mechanism.

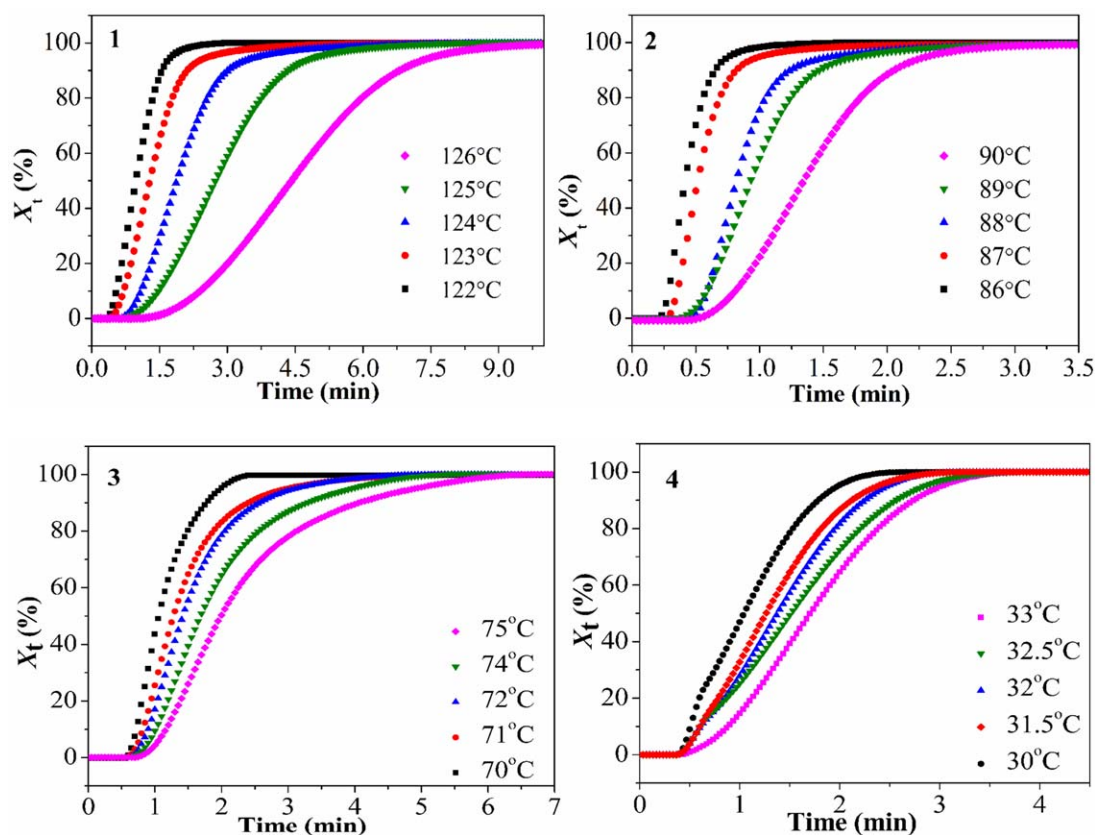


Figure 4. Relative crystallinity versus crystallization time at different crystallization temperatures for HBPEs. [Color figure can be viewed in the online issue, which is available at wileyonlinelibrary.com.]

Table I. Isothermal Crystallization Kinetic Parameters of HBPEs at Different Crystallization Temperatures

| Sample | T_c (°C) | $t_{1/2}$ (min) | n | $\ln K$ | K (min $^{-n}$) | t_{max} (min) | $\tau_{1/2}$ (min) |
|--------|------------|-----------------|------|----------|--------------------|-----------------|--------------------|
| 1 | 122 | 0.98 | 2.61 | -0.30935 | 0.7339 | 0.94 | 1.02 |
| | 123 | 1.28 | 2.43 | -0.9680 | 0.3798 | 1.20 | 0.78 |
| | 124 | 1.88 | 2.59 | -2.0007 | 0.1352 | 1.79 | 0.53 |
| | 125 | 2.75 | 2.61 | -3.00979 | 0.0493 | 2.63 | 0.36 |
| | 126 | 4.35 | 2.96 | -4.70909 | 0.0090 | 4.17 | 0.23 |
| 2 | 86 | 0.42 | 2.76 | 2.045 | 7.7292 | 0.40 | 2.40 |
| | 87 | 0.51 | 2.71 | 1.44708 | 4.2507 | 0.49 | 1.96 |
| | 88 | 0.81 | 2.95 | 0.2527 | 1.2875 | 0.80 | 1.23 |
| | 89 | 0.93 | 2.70 | -0.1749 | 0.8395 | 0.90 | 1.07 |
| | 90 | 1.34 | 2.93 | -1.22323 | 0.2943 | 1.32 | 0.75 |
| 3 | 70 | 1.04 | 2.01 | -0.43096 | 0.6499 | 0.88 | 0.96 |
| | 71 | 1.27 | 2.09 | -0.8500 | 0.4274 | 1.10 | 0.79 |
| | 72 | 1.41 | 2.08 | -1.08086 | 0.3393 | 1.23 | 0.71 |
| | 74 | 1.68 | 2.01 | -1.4218 | 0.2413 | 1.44 | 0.59 |
| | 75 | 1.99 | 2.03 | -1.8142 | 0.1630 | 1.75 | 0.50 |
| 4 | 30 | 1.04 | 2.19 | -0.4549 | 0.6345 | 0.93 | 0.96 |
| | 31.5 | 1.27 | 2.32 | -0.91313 | 0.4013 | 1.16 | 0.79 |
| | 32 | 1.42 | 2.21 | -1.1409 | 0.3195 | 1.28 | 0.70 |
| | 32.5 | 1.51 | 2.25 | -1.29049 | 0.2751 | 1.37 | 0.66 |
| | 33 | 1.71 | 2.54 | -1.72243 | 0.1786 | 1.62 | 0.59 |

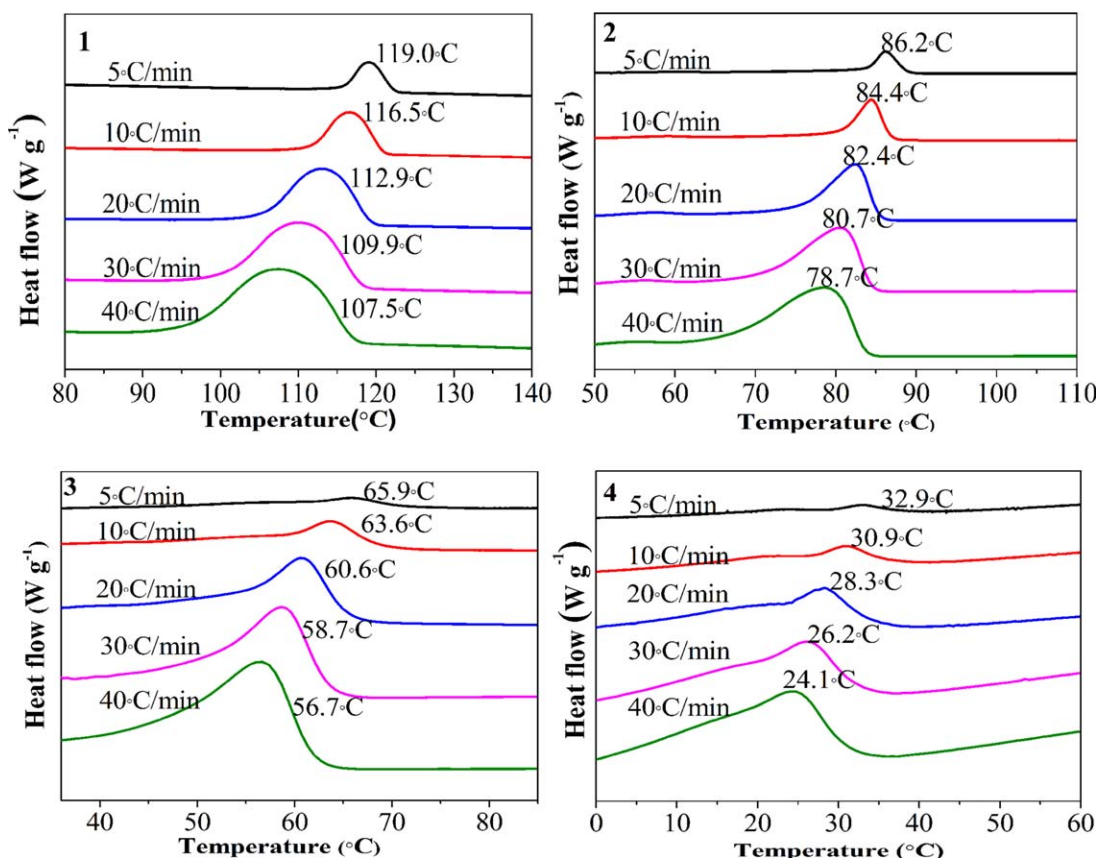


Figure 5. DSC curves of non-isothermal melt crystallization for HBPEs at the indicated cooling rates. [Color figure can be viewed in the online issue, which is available at wileyonlinelibrary.com.]

The DB of HBPE2 was 0.110 and higher than that of HBPE1 (DB = 0). However, $\tau_{1/2}$ value of HBPE2 was higher than that of HBPE1, which indicated the crystallization rate of HBPE2 was higher than that of HBPE1. In other words, the small amount of branch structure in HBPE2 could improve its crystallization rate. This might be attributed to the self-nucleation effect of the lower branch content.^{35,40,46,47} A slight amount of branch content can play a role of heterogeneous nucleation agent in the slow nucleation stage and accelerate the crystallization process. On the contrary, the DB values of HBPE3 and HBPE4 were 0.186 and 0.258 respectively, which meant the branch content was high enough. Their $\tau_{1/2}$ values were lower than that of HBPE1 and indicated lots of branch content could inhibit the crystallization process of the polymer. Thus the crystallization was decreased obviously.

Non-Isothermal Crystallization Kinetics

The DSC thermograms of non-isothermal crystallization for HBPEs at different cooling rates ranging from 5 to 40 °C/min were presented in Figure 5. All HBPE samples showed a single crystallization peak in DSC curves and the crystallization peak temperature (T_p) decreased with increasing cooling rate. For example, the T_p of HBPE1 (linear polyethylene) at a cooling rate of 5 °C/min was 117.5 °C, while at a cooling rate of 40 °C/min, it was almost 10 °C lower. At the same time, the range of crystallization temperature became boarder, which indicated the cooling rate could affect the nucleation and crystal growth of

HBPEs significantly. T_p of HBPE1 was higher than that of other three HBPEs at the same cooling rate, which indicated that the HBPEs with high DB was more difficult to crystallize during the scanning. Comparing the T_p of HBPE1 at the different cooling rate, it shifted to low temperature as increasing the cooling rate. This implied that there was not enough time to activate the nuclei at high temperature when crystallized at high cooling rate, and the imperfect crystal structures formed at rapid cooling rates.³⁴ A similar trend was also observed in the other three HBPEs.

Relative crystallinity at every crystallization temperature (X_t) could be formulated by the following relation:

$$X_t = \frac{\int_{t_0}^t (dH/dt) dt}{\int_{t_0}^{t_\infty} (dH/dt) dt} \quad (6)$$

Where dH/dt was the rate of heat evolution, ΔH_t was the total heat evolved at time t , and ΔH_∞ was the total heat evolved at completion. Values t_0 and t_∞ were the time at which the crystallization process started and ended, respectively.

Plots of relative crystallinity versus temperature were shown in Supporting Information Figure S3. Obviously the crystallization process of each sample could be divided into three stages: slow nucleation stage, fast primary crystallization stage, and slow secondary crystallization stage.

In non-isothermal crystallization process, the relationship of t , T , and R could be expressed as:

$$t = (T_0 - T)R \quad (7)$$

Where T_0 was the initial crystallization temperature, T was the crystallization temperature at time t and R was the cooling rate. Therefore, curves of X_t versus T could be converted into curves of X_t versus t , which were shown in Supporting Information Figure S4. With the increase of cooling rate, the crystallization time required decreased. At a given cooling rate, the crystallization time decreased first and increased then with the increase of DB, which indicated that branch structure could inhibit crystallization. However, once crystallization began, little branched structure could accelerate the crystallization, which was in accordance with the result of isothermal crystallization.

Avrami method could also be used to analysis the non-isothermal crystallization of polymer. However, many scholars developed several new methods based on Avrami equation [eq. (2)]. For example, Ozawa assumed that the non-isothermal crystallization process was composed of infinite small isothermal crystallization steps and extended the Avrami equation to the non-isothermal process. Ozawa's theory can be expressed as:

$$1 - X_t = \exp[-K(T)/R^m] \quad (8)$$

Where X_t was the relative degree of crystallinity at temperature T , $K(T)$ was the cooling crystallization function, R was the cooling rate, and m was the Ozawa exponent which was related to the mechanism of nucleation and dimension of crystal growth. Equation (8) could be rewritten as:

$$\ln[-\ln(1 - X_t)] = \ln K(T) - m \ln R \quad (9)$$

By plotting $\ln[-\ln(1 - X_t)]$ against $\ln R$, a straight line was obtained if the Ozawa method was valid and then kinetics parameters (m and $K(T)$) could be derived from the slope and the intercept, respectively. As shown in Supporting Information Figure S5, non-linear relation was found for the non-isothermal crystallization process of the four samples. Therefore, the Ozawa equation could not describe the non-isothermal crystallization process of HBPEs. Because the procedure of non-isothermal crystallization was a dynamic process, and the crystallization rate was no longer constant but a function of time and cooling rate.⁴⁸ Furthermore, Ozawa did not take into consideration of recrystallization and the dependence of the fold length on temperature in his approach.⁴⁹

Mo *et al.* developed a new model for non-isothermal crystallization kinetics by combining the Avrami equation with the Ozawa equation. In this case, the relationship of t , K and R can be expressed as:

$$\ln Z_t + n \cdot \ln t = \ln K(t) - m \cdot \ln R \quad (10)$$

where $F(T) = [K(T)/Z_t]^{1/m}$ is defined as the cooling rate to obtain a certain relative crystallinity in one unit of time, representing the crystallization rate of polymers. Here $\alpha = n/m$, in which n and m are the Avrami exponent and the Ozawa exponent, respectively. Therefore, the following equation can be obtained at a given crystallinity degree:

$$\ln R = \ln F(T) - \alpha \ln t \quad (11)$$

According to eq. (11), a good linear relationship between $\ln R$ and $\ln t$ for the HBPE samples at a given crystallinity degree

Table II. Values of $F(T)$ and α for HBPEs with Different DB

| Sample | X_t (%) | $\ln F(T)$ | $F(T)$ | α |
|--------|-----------|------------|--------|----------|
| 1 | 10 | 2.16 | 8.67 | 1.20 |
| | 30 | 2.40 | 11.02 | 1.15 |
| | 50 | 2.55 | 12.81 | 1.22 |
| | 70 | 2.74 | 15.49 | 1.28 |
| | 90 | 2.93 | 18.73 | 1.35 |
| 2 | 10 | 0.89 | 2.44 | 1.54 |
| | 30 | 1.38 | 3.97 | 1.55 |
| | 50 | 1.67 | 5.31 | 1.49 |
| | 70 | 1.90 | 6.69 | 1.46 |
| | 90 | 2.19 | 8.94 | 1.42 |
| 3 | 10 | 2.49 | 12.06 | 1.76 |
| | 30 | 2.72 | 15.18 | 1.65 |
| | 50 | 2.87 | 17.64 | 1.60 |
| | 70 | 3.02 | 20.49 | 1.58 |
| | 90 | 3.24 | 25.53 | 1.57 |
| 4 | 10 | 2.74 | 15.49 | 1.26 |
| | 30 | 2.85 | 17.29 | 1.28 |
| | 50 | 2.95 | 19.11 | 1.32 |
| | 70 | 3.07 | 21.54 | 1.36 |
| | 90 | 3.27 | 26.31 | 1.28 |

appeared as shown in Supporting Information Figure S6. The intercept and the slope obtained from the line represent $F(T)$ and α respectively, which are listed in Table II. It can be seen that the values of $F(T)$ continuously increase with increasing crystallinity, and the α value slightly changed for each sample. Therefore, a relatively high cooling rate should be selected in order to achieve a high degree of crystallinity at a fixed crystallization time. In addition, at a given crystallinity, the $F(T)$ values increase with increasing DB except for HBPE2, which is smaller than that of other three samples, indicating that the introduction of small amount of branching architecture can accelerate the crystallization rate. Wherever, with further increase the DB, the crystallization process would be hindered, which is consistent with the result from isothermal crystallization. In a short, Mo' equation successfully described the non-isothermal crystallization process of HBPEs.

CONCLUSIONS

A series of HBPEs with different DB were used to investigate their melt behavior and crystallization kinetics in isothermal and non-isothermal crystallization process. The results showed a slight amount of branch structure might accelerate the crystallization rate, but the high content of branch structure could inhibit the crystallization process of HBPEs. The equilibrium melting point of the four HBPEs were 152.4 °C, 139.8 °C, 92.9 °C, and 53.2 °C, respectively determined by Hoffmann-Weeks method. They decreased with increasing DB, which implied the thickness of the HBPE crystal plate decreased with increasing the DB. Isothermal crystallization of HBPEs was described by the Avrami equation and non-isothermal crystallization of HBPEs under consideration was investigated by two

methods: the Ozawa method and the relation deduced by Mo. However, Ozawa method was failed to describe the non-isothermal crystallization, and Mo's equation could be used to describe the non-isothermal crystallization process well.

ACKNOWLEDGMENTS

This work was supported by the National Basic Research Program (No. 2012CB821500) and the National Natural Science Foundation of China (No. 91127047).

REFERENCES AND NOTES

- Zheng, Y.; Li, S.; Weng, Z.; Gao, C. *Chem. Soc. Rev.* **2015**, *44*, 4091.
- Liu, Y.; Huang, Z.; Liu, K.; Kelgtermans, H.; Dehaen, W.; Wang, Z.; Zhang, X. *Polym. Chem.* **2014**, *5*, 53.
- Buonocore, G. G.; Schiavo, L.; Attianese, I.; Borriello, A. *Compos. Part B: Eng.* **2013**, *53*, 187.
- Tan, J. H.; McMillan, N. A. J.; Payne, E.; Alexander, C.; Heath, F.; Whittaker, A. K.; Thurecht, K. J. *J. Polym. Sci. Part A: Polym. Chem.* **2012**, *50*, 2585.
- Malinova, K.; Gunesch, M.; Pancera, S. M.; Wengeler, R.; Rieger, B.; Volkmer, D. *J. Colloid. Interf. Sci.* **2012**, *374*, 61.
- Shepherd, J.; Sarker, P.; Rimmer, S.; Swanson, L.; MacNeil, S.; Douglas, I. *Biomaterials* **2011**, *32*, 258.
- Larrazza, I.; Peinado, C.; Abrusci, C.; Catalina, F.; Corrales, T. *J. Photochem. Photobiol. A: Chem* **2011**, *224*, 46.
- Dong, R.; Liu, Y.; Zhou, Y.; Yan, D.; Zhu, X. *Polym. Chem* **2011**, *2*, 2771.
- Zhou, Y.; Huang, W.; Liu, J.; Zhu, X.; Yan, D. *Adv. Mater.* **2010**, *22*, 4567.
- Fogelström, L.; Malmström, E.; Johansson, M.; Hult, A. *ACS Appl. Mater. Inter.* **2010**, *2*, 1679.
- Sangermano, M.; Messori, M.; Galleco, M. M.; Rizza, G.; Voit, B. *Polymer* **2009**, *50*, 5647.
- Liu, F.; Liu, J. Q.; Liu, R. R.; Hou, X. Y.; Xie, L. H.; Wu, H. B.; Tang, C.; Wei, W.; Cao, Y.; Huang, W. *J. Polym. Sci. Part A: Polym. Chem.* **2009**, *47*, 6451.
- Ratna, D. *J. Adhes. Sci. Technol.* **2008**, *22*, 101.
- Zou, J.; Shi, W.; Hong, X. *Compos. Part A: Appl. Sci. Manuf.* **2005**, *36*, 631.
- Wong, S.; Shanks, R. A.; Hodzic, A. *Macromol. Mater. Eng.* **2004**, *289*, 447.
- Mezzenga, R.; Boogh, L.; Månson, J. A. E. *Compos. Sci. Technol.* **2001**, *61*, 787.
- Halter, D.; Frey, H. *Acta Polym.* **1997**, *48*, 298.
- Tinetti, S. M.; Faulkner, B. J.; Nelson, R. M.; Priddy, D. B. *J. Appl. Polym. Sci.* **1997**, *64*, 683.
- Jayakannan, M.; Ramakrishnan, S. *J. Polym. Sci., Part A: Polym. Chem* **1998**, *36*, 309.
- Litvinenko, G. I.; Simon, P. F. W.; Müller, A. H. E. *Macromolecules* **1999**, *32*, 2410.
- Jikei, M.; Kakimoto, M. *Prog. Polym. Sci.* **2001**, *26*, 1233.
- Gong, W.; Mai, Y.; Zhou, Y.; Qi, N.; Wang, B.; Yan, D. *Macromolecules* **2005**, *38*, 9644.
- Zhu, X.; Zhou, Y.; Yan, D. *J. Polym. Sci. Part B: Polym. Phys.* **2011**, *49*, 1277.
- Lee, J. S.; Quirk, R. P.; Foster, M. D. *Macromolecules* **2005**, *38*, 5381.
- Luo, X.; Xie, S.; Liu, J.; Hu, H.; Jiang, J.; Huang, W.; Gao, H.; Zhou, D.; Lü, Z.; Yan, D. *Polym. Chem.* **2014**, *5*, 1305.
- Geifer, M. Y.; Winter, H. H. *Macromolecules* **1999**, *32*, 8974.
- Chae, H. G.; Kim, B. C.; Im, S. S.; Han, Y. K. *Polym. Eng. Sci.* **2001**, *41*, 1133.
- Chiu, F. C.; Peng, Y.; Fu, Q. *J. Polym. Res.* **2002**, *9*, 175.
- Zhang, F.; Liu, J.; Fu, Q.; He, T. *Acta Polym. Sin.* **2000**, 725.
- Zhang, X. B.; Li, Z. S.; Lu, Z. Y.; Sun, C. C. *Macromolecules* **2002**, *35*, 106.
- Mai, Y.; Zhou, Y.; Hou, J. *New J. Phys.* **2005**, *7*, 1.
- Krishnaswamy, R. K.; Yang, Q.; Fernandez-Ballester, L.; Kornfield, J. A. *Macromolecules* **2008**, *41*, 1693.
- Nozue, Y.; Kawashima, Y.; Seno, S.; Nagamatsu, T.; Hosoda, S.; Berda, E. B.; Rojas, G.; Baughman, T. W.; Wagener, K. B. *Macromolecules* **2011**, *44*, 4030.
- Yang, B.; Yang, M.; Wang, W. J.; Zhu, S. *Polym. Eng. Sci.* **2012**, *52*, 21.
- Wang, L.; Jiang, Z. W.; Liu, F.; Zhang, Z. J.; Tang, T. *Chin. J. Polym. Sci.* **2014**, *32*, 333.
- Hosoda, S.; Nozue, Y.; Kawashima, Y.; Suita, K.; Seno, S.; Nagamatsu, T.; Wagener, K. B.; Inci, B.; Zuluaga, F.; Rojas, G.; Leonard, J. K. *Macromolecules* **2011**, *44*, 313.
- Inci, B.; Lieberwirth, I.; Steffen, W.; Mezger, M.; Graf, R.; Landfester, K.; Wagener, K. B. *Macromolecules* **2012**, *45*, 3367.
- Rojas, G.; Inci, B.; Wei, Y.; Wagener, K. B. *J. Am. Chem. Soc.* **2009**, *131*, 17376.
- Matsui, K.; Seno, S.; Nozue, Y.; Shinohara, Y.; Amemiya, Y.; Berda, E. B.; Rojas, G.; Wagener, K. B. *Macromolecules* **2013**, *46*, 4438.
- He, F. A.; Zhang, L. M. *Polym. Test* **2014**, *35*, 80.
- Xenopoulos, A.; Wunderlich, B. *J. Polym. Sci. Part B: Polym. Phys.* **1990**, *28*, 2271.
- Franco, L.; Puiggali, J. *J. Polym. Sci. Part B: Polym. Phys.* **1995**, *33*, 2065.
- Li, Y.; Zhu, X.; Tian, G.; Yan, D.; Zhou, E. *Polym. Int.* **2001**, *50*, 677.
- Hoffman, J. D.; Weeks, J. J. *J. Res. Natl. Bur. Stand* **1962**, *66A*, 13.
- Jonsson, H.; Wallgren, E.; Hult, A.; Gedde, U. W. *Macromolecules* **1990**, *23*, 1041.
- Tian, J.; Yu, W.; Zhou, C. *J. Appl. Polym. Sci.* **2007**, *104*, 3592.
- Naguib, H. E.; Park, C. B.; Song, S. W. *Ind. Eng. Chem. Res.* **2005**, *44*, 6685.
- Weng, W.; Chen, G.; Wu, D. *Polymer* **2003**, *44*, 8119.
- Börjesson, L.; Stevens, J. R.; Torell, L. M. *Polymer* **1987**, *28*, 1803.